

## Aberystwyth University

### *8000 years of North Atlantic storminess reconstructed from a Scottish peat record: implications for Holocene atmospheric circulation patterns in Western Europe*

Stewart, Helena; Bradwell, Tom; Bullard, Joanna E.; Davies, Sarah; McCulloch, Robert

*Published in:*

Journal of Quaternary Science

*DOI:*

[10.1002/jqs.2983](https://doi.org/10.1002/jqs.2983)

*Publication date:*

2017

*Citation for published version (APA):*

Stewart, H., Bradwell, T., Bullard, J. E., Davies, S., & McCulloch, R. (2017). 8000 years of North Atlantic storminess reconstructed from a Scottish peat record: implications for Holocene atmospheric circulation patterns in Western Europe. *Journal of Quaternary Science*, 32(8), 1075-1084. <https://doi.org/10.1002/jqs.2983>

#### **General rights**

Copyright and moral rights for the publications made accessible in the Aberystwyth Research Portal (the Institutional Repository) are retained by the authors and/or other copyright owners and it is a condition of accessing publications that users recognise and abide by the legal requirements associated with these rights.

- Users may download and print one copy of any publication from the Aberystwyth Research Portal for the purpose of private study or research.
- You may not further distribute the material or use it for any profit-making activity or commercial gain
- You may freely distribute the URL identifying the publication in the Aberystwyth Research Portal

#### **Take down policy**

If you believe that this document breaches copyright please contact us providing details, and we will remove access to the work immediately and investigate your claim.

tel: +44 1970 62 2400

email: [is@aber.ac.uk](mailto:is@aber.ac.uk)

1 **8000 years of North Atlantic storminess reconstructed from a Scottish peat record:**  
2 **implications for Holocene atmospheric circulation patterns in Western Europe**

3

4 H. Stewart,<sup>1</sup> T. Bradwell,<sup>1</sup> J. Bullard,<sup>2</sup> S.J. Davies,<sup>3</sup> N. Golledge<sup>4</sup> and R.D. McCulloch<sup>1\*</sup>

5 <sup>1</sup> Biological & Environmental Sciences, University of Stirling, Stirling, FK9 4LA, Scotland, UK.

6 <sup>2</sup> Department of Geography, Loughborough University, Loughborough, LE11 3TU, England,  
7 UK.

8 <sup>3</sup> Department of Geography and Earth Sciences, Aberystwyth University, SY23 3DB, Wales,  
9 UK.

10 <sup>4</sup> Antarctic Research Centre, Victoria University of Wellington, Wellington 6140, New  
11 Zealand.

12

13 \*Corresponding author: [robert.mcculloch@stir.ac.uk](mailto:robert.mcculloch@stir.ac.uk)

14

15 ABSTRACT: North Atlantic storminess can affect human settlements, infrastructure and  
16 transport links, all of which strongly impact local, national and global economies. An  
17 increase in storm frequency and intensity is predicted over the Northeast Atlantic in the 21<sup>st</sup>  
18 century because of a northward shift in storm tracks and a persistently positive North  
19 Atlantic Oscillation (NAO), driven by recent atmospheric warming. Although documentary  
20 records of North Atlantic storminess exist, these are generally limited to the last c. 1000-  
21 2000 years. This paper presents a continuous high-resolution proxy record of storminess  
22 spanning the last 8000 years from a 6 m long core taken from a peat bog in Northern  
23 Scotland. Bromine concentrations in the peat, derived from sea spray, are used to  
24 reconstruct storm frequency and storm intensity, and mire surface wetness is used as an

25 indicator of longer-term climate shifts. The results suggest a relationship between positive  
26 phases of the NAO and increased North Atlantic storminess. However, subtle differences  
27 between bromine concentrations and mire surface wetness suggest that high intensity but  
28 perhaps less frequent periods of storminess are not necessarily associated with a wetter  
29 climate.

30

31 KEYWORDS: Holocene storminess; NAO; micro-XRF; mire surface wetness; Scotland.

32

### 33 **Introduction**

34 The location and intensity of mid-latitude storm tracks strongly influence the climate of  
35 Europe (Hanna *et al.*, 2008). The most intense and damaging storms affecting Europe  
36 originate in the North Atlantic, often causing extensive flooding and damage to  
37 infrastructure, and resulting in significant detrimental economic impacts. The highest  
38 magnitude storms occur most frequently during winter, when the storm tracks are most  
39 intense, and extend in a north-westerly direction from the east coast of North America, to  
40 Ireland, Great Britain and Norway (Cheng *et al.*, 2011). North Atlantic storminess has  
41 increased over recent decades in association with warming air temperatures over the same  
42 period (Alexander and Tett, 2005, Allan *et al.*, 2009, Wang *et al.*, 2009). Predictions suggest  
43 that over the next 100 years North Atlantic storm tracks will shift northwards and storm  
44 frequency will increase in the British Isles due to an intensified jet stream (Pinto *et al.*, 2009;  
45 Orme *et al.*, 2015).

46

47 Records of past storminess have been reconstructed through both observational and  
48 sedimentary (or palaeoenvironmental) records. Observational records tend to span the past  
49 few hundred years and are based on air temperature (Dawson *et al.*, 2003), sea surface  
50 temperature (Hurrell, 1995) and wind speed (Clarke and Rendell, 2009; Dawson *et al.*,  
51 2010). In Europe and the North East Atlantic, proxy measures for increased wind strength  
52 include aeolian sand influx (de la Vega-Leinert *et al.*, 2000; Clarke *et al.*, 2002; Sommerville  
53 *et al.*, 2003; de Jong *et al.*, 2006; Clarke and Rendell, 2009; Tisdall *et al.*, 2013), over-wash  
54 deposits in coastal lagoons (Sabatier *et al.*, 2012), cliff-top storm deposits left by extreme  
55 waves (Hansom and Hall, 2009), marine records reflecting wind-blown current strength and  
56 storm deposits (Hass, 1996; Andresen *et al.*, 2005). and Na<sup>+</sup> from the Greenland ice cores  
57 (Dawson *et al.*, 2003). Paleoenvironmental reconstructions of North Atlantic storminess  
58 tend to span from the mid-Holocene to the present and so high-resolution records on a  
59 millennial timescale (10<sup>3</sup> a) are an important goal in order to gauge longer-term trends and  
60 better understand Holocene climate variability.

61

62 The position and strength of the polar front jet stream in the Northern Hemisphere strongly  
63 determines the process of cyclogenesis between ~40 and 65°N, and, therefore, the number  
64 and frequency of high-energy storms in the North Atlantic region (Fig. 1). The development  
65 of a vigorous jet stream in winter, enabled by strong temperature contrasts between mild  
66 moist mid-latitude and cold polar air, accounts for the strength and trajectory of dominant  
67 westerly winds as well as the frequency of extra-tropical storms and their tracks over north-  
68 western Europe (Hurrell 1995, Hurrell *et al.*, 2003; Athanasiadis *et al.*, 2010). Secular changes  
69 in the North Atlantic Oscillation (NAO), defined as the sea-level pressure difference between  
70 the main North Atlantic pressure dipole measured in Iceland and the Azores, are strongly

71 associated with changes in the polar-front jet stream (Hurrell 1995; Woollings *et al.*, 2008,  
72 2010). An enhanced NAO (positive) mode typically results from undisturbed strong zonal (east  
73 to west) jet stream flow between 50 and 60°N; whilst a negative NAO mode results from  
74 disturbed, meridional flow with a large north-south component leading to blocking highs and  
75 cut-low pressure systems. During a negative NAO, the dominant westerly winds often follow  
76 a more southern trajectory owing to the development of a large quasi-stationary high-  
77 pressure system over Greenland (Woollings *et al.*, 2008, 2010). Both strongly positive and  
78 negative NAO modes represent end members and require relatively vigorous jet-stream-  
79 driven atmospheric circulation in the North Atlantic sector. These conditions are normally  
80 optimised during European winter, hence the strong positive correlation between NAO mode  
81 and winter precipitation in NW Britain and western Norway (Hurrell, 1995; Hurrell *et al.*,  
82 2003). However, other more subdued long-term synoptic situations can occur. These include  
83 a neutral NAO phase, where the pressure index is neither strongly positive nor strongly  
84 negative, normally associated with a weakening of the main Iceland cyclonic and Azores  
85 anticyclonic pressure systems. In this situation, the development of large persistent  
86 Scandinavian high-pressure systems can block the path of westerly winds into NW Europe,  
87 further reducing cyclonic activity and dampening the NAO index into a more neutral state  
88 (Mauri *et al.*, 2014).

89

90 This paper presents chemical variability and palaeo-moisture indices from a six metre-long  
91 peat core in maritime Northern Scotland. Analyses of down-core variations in bromine  
92 concentrations as an indicator of storm intensity are coupled with mire surface wetness  
93 (MSW) as an indicator of longer-term storm-track position and climate shifts in the

94 Northeast Atlantic. Finally, we compare our record to other proxies for shifts in the NAO  
95 during the Holocene.

96

## 97 Bromine as an indicator of storminess

98 The generation of sea-salt aerosol is the principal global source of atmospheric Br,  
99 producing  $\sim 6.2$  Tg/a (Sanders *et al.*, 2003). The bursting of air bubbles and the direct  
100 formation of droplets by wave crests injects sea-salt aerosol into the atmosphere and so the  
101 flux of Br is dependent on wind speed (Moldanová and Ljungström, 2001). Marine aerosols  
102 may be transported long distances (10s-100s km) and be dry deposited or scavenged from  
103 the atmosphere by rainfall (Gustafsson and Franzén, 2000). Other sources of inorganic Br  
104 are dust, biomass-burning and fossil fuels but these are of an order of magnitude less than  
105 marine sources. Crustal sources are estimated to be 4% of the global Br flux and its  
106 deposition is geographically restricted to the equatorial Atlantic and North Pacific Oceans  
107 (Sanders *et al.*, 2003). Ombrotrophic peat bogs receive only atmospheric inputs and so  
108 provide excellent archives of climatic change. It has been argued that Br concentrations are  
109 determined by climate-controlled biogenic processes (Biester *et al.*, 2004; Moreno *et al.*,  
110 2015) and are not stratigraphically retained. However, other studies have demonstrated  
111 that Br is stably retained in the humic acid content of peat and down-core variations are  
112 conserved (Zaccone *et al.*, 2008; Orme *et al.*, 2015; Turner *et al.*, 2015). Br concentrations in  
113 peat bogs around the maritime fringes of the North Atlantic, such as in the British Isles, are  
114 very likely to be derived from sea spray; hence higher Br levels suggest an increase in sea  
115 turbulence, accentuated wave action, and increased windiness during storms. Mire surface  
116 wetness (MSW), an additional measure, indicates longer-term changes in precipitation

117 patterns with increased MSW signalling a more persistent wetter climate (Charman *et al.*,  
118 2006; Turner *et al.*, 2014).

119

## 120 **Materials and methods**

### 121 Site description and field sampling

122 A continuous high-resolution peat core (to 6.08 m depth) was obtained from the central  
123 part of a large mire at Shebster, northern Caithness (58°33'06.6" N, 003°42'39.0" W; 82 m  
124 asl; 4.8km from the North Atlantic coast) (Fig. 2). The mire surface is bordered by the Burn  
125 of Shebster that drains northwards. The bedrock underlying the site is Middle Devonian  
126 sandstone of the Bighouse Formation (Auton *et al.*, 2005). The core was sampled from  
127 within the deepest part of the Shebster peat bog using a 1-metre long (75 mm diameter)  
128 Russian D-section sampler (with 10 cm overlapping sections). Recovered cores were  
129 transferred into plastic guttering, sealed in lay-flat tubing, and stored at the University of  
130 Stirling at a constant temperature of 4°C.

131

### 132 Minerogenic analysis

133 The core was sub-sampled in contiguous 2cm<sup>3</sup> sections for acid digestion to remove organic  
134 matter (c.f. Dugmore *et al.*, 1995a). The mineral residue was then scanned using light  
135 microscopy to identify tephra glass shards to supplement the radiocarbon chronology with  
136 tephrochronology.

137

### 138 Organic content

139 To provide a record of bio-productivity and organic content, contiguous samples of 2 cm  
140 depth were combusted in a muffle furnace at 550°C for 4 hours to enable the calculation of  
141 the percentage loss-on-ignition (LOI<sub>550</sub>).

142

143 Mire surface wetness

144 The degree of peat humification, as a proxy of MSW, was estimated using the colorimetric  
145 alkali extract method modified from Blackford (1993). Under drier conditions peat is more  
146 oxidised, the accumulation rate is slower and there is an increase in humic material. The  
147 greater the humic content the darker the extract solution and the lower the transmitted  
148 light values. Therefore, lower percentage transmission values indicate drier peat  
149 accumulation conditions whereas higher percentage transmission values indicate wetter  
150 conditions. Contiguous sub-samples of 2 cm<sup>3</sup> were taken from the 608 cm core. Samples  
151 were oven dried at 80°C for 24 hrs and then ground using a small rotating blade grinder.  
152 Sub-samples of 0.2 g were placed into 50 ml falcon centrifuge tubes and 50 ml of NaOH 8%  
153 w/v was added to each sample and the tubes placed in a boiling water bath for 60 minutes  
154 and intermittently stirred. The samples were then centrifuged at 3000 rpm for 5 minutes  
155 and a 0.5 ml aliquot pipetted into a 10 mm cuvette and 2.5 ml of distilled water added. The  
156 cuvettes were analysed in a Thermo Scientific Genesys 20 spectrophotometer and the  
157 percentage transmitted light measured at 540 nm. This method allowed for batches of 20  
158 samples to be analysed in under 30 min. from removal from the water bath and so minimise  
159 any fading of the solution (cf. Blackford, 1993).

160

161 Micro X-Ray Fluorescence Geochemistry



162 The core was analysed using an Itrax<sup>®</sup> X-Ray Fluorescence core scanner at Aberystwyth  
163 University. Non-destructive elemental analysis, including Br was performed at 2mm  
164 intervals using a molybdenum (Mo) anode X-ray tube (settings: 30 kV, 50 mA, count time 10  
165 seconds). The results are expressed as a ratio of the coherent+incoherent (coh/incoh)  
166 values, which are used as proxies for organic and moisture content. The coh/incoh ratio  
167 minimises any influence from these proxies on the geochemical data. Density and colour  
168 information was further obtained using X-radiography and digital RGB optical imagery.

169

## 170 Chronology

171 Five samples of wood material were AMS radiocarbon dated to enable the construction of a  
172 Bayesian age-depth model. All samples were pre-treated with an acid/alkali/acid treatment.  
173 To augment the radiocarbon chronology, a cryptotephra layer (346 cm depth) was analysed  
174 through the geochemical fingerprinting of individual shards by the SX100 Cameca Electron  
175 microprobe at the University of Edinburgh using methods established by Hunt and Hill  
176 (1993) and Hayward (2013).

177

178 The cryptotephra at 346 cm is geochemically correlated to the eruption of Hekla 4  
179 (Tephabase; Newton, 1996) and provides an isochronic marker dated to  $3826 \pm 12$  <sup>14</sup>C a BP  
180 (Dugmore *et al.* 1995b). The AMS radiocarbon and tephra ages were calibrated using Calib  
181 ver.7.10 (Stuiver and Reimer, 1993) and IntCal13 (Reimer *et al.*, 2013)(Table 1). The  
182 Bayesian program, BACON v2.2 (Blaauw and Christen, 2011) was used to construct an age-  
183 depth model to constrain the stratigraphic results (Fig. 3). The age-depth model indicates a  
184 mean accumulation rate of 13 yrs/cm and a uniform rate of peat accumulation during the  
185 Holocene.

186

## 187 **Results**

188 From 612 to 608 cm depth greyish-brown organic mud grades to a dark brown moderately  
189 humified peat (with wood fragments at 404 – 406 cm depth) that continues to ~370 cm.

190 From ~ 370 to 271 cm, the core comprises very dark brown well-humified amorphous peat.

191 At 271 cm, there is a marked transition to a dark brown peat with abundant sedge

192 fragments. The sedge-rich peat continues to 27 cm and is moderately well humified and

193 with occasional wood fragments. From 27 cm to the surface root mat, the core comprises a

194 dark brown fibrous sphagnum peat.

195

196 To aid the interpretation, the Shebster stratigraphic data is divided into 8 major zones based

197 on major changes in the MSW as this is a site-specific proxy (Fig. 3).

198

199 SH-1 8210 – 7400 cal a BP: MSW was not measured in the lowest ~10 cm of the peat to

200 avoid any potential influence from the underlying lake sediments; measurements

201 commenced at 590 cm. In Zone SH-1 the MSW curve is characterised by two peaks at c.

202 7960 and 7610 cal a BP, separated by a nadir at c. 7740 cal a BP. The Br ratios appear to be

203 in antiphase with the largest peak of the entire record occurring at c. 7800 cal a BP, before

204 both MSW and bromine decline to a low at the upper zone boundary at c. 7400 cal a BP.

205

206 SH-2 7400 - 5270 cal a BP: At the start of this zone there is a marked step up to higher MSW

207 values that fluctuate (between ~20 and 30 %T) through the first half of the zone. Br values

208 commence from a peak between c. 7400 and 7300 cal a BP and then decline to a broad low

209 also during the first half of the zone, between c. 7300 and 6200 cal a BP. At c. 6145 cal a BP  
210 there is a rapid increase in Br to a sustained peak until a fall at c. 5700 to lower but  
211 fluctuating values and then increasing towards the upper zone boundary. The MSW values  
212 in the second half of the zone also continue to fluctuate (between ~25 and 35 %T) but at  
213 higher values than previously.

214

215 SH-3 5200 - 4000 cal a BP: Br increase to a peak between c. 5200 and 4900 cal a BP followed  
216 by a sustained declining trend towards the upper zone boundary at c. 4000 cal a BP. The  
217 decline in Br is reflected in a similar profile in the MSW, excepting a brief minor peak in  
218 MSW at c. 4540 cal a BP.

219

220 SH-4 4000 - 3300 cal a BP: The Br ratios reach their minima at c. 3850 cal a BP and remain  
221 relatively stable before gradually increasing from c. 3400 cal a BP to a peak at the upper  
222 zone boundary. During this zone the stratigraphy changes to well-humified peat and this is  
223 reflected in the sharp fall of MSW values where they reach their lowest values of the entire  
224 record before rising again at the top of the zone.

225

226 SH-5 3300 – 2400 cal a BP: MSW values rise to a peak at c. 3160 cal a BP (25.6 %T) and  
227 continue to rise to ~30%, punctuated by a brief decline to 17.5 %T at c. 3005 cal a BP. Br  
228 values remain relatively stable, with small fluctuations occurring throughout this period.

229

230 SH-6 2400 - 1400 cal a BP: MSW values fluctuate between ~33 and 20 %T during this zone  
231 and Br values continue to be relatively stable.

232

233 SH-7 1400 – 600 cal a BP: Br ratios peak between c. 1225 and 1130 cal a BP and between c.  
234 855 and 750 cal a BP before declining to a low at c. 600 cal a BP. MSW values increase to a  
235 peak at c. 1365 cal a BP (39.1 %T) then decline to a low at c. 1115 cal a BP (18.0 %T)  
236 followed by peaks at c. 950 (34.1 %T) and 675 cal a BP (34.8 %T).

237

238 SH-8 600-0 cal a BP: MSW values decline to a low at c. 300 cal a BP (18.8 %T) before rising to  
239 a peak of 43.3 %T at c. 140 cal a BP. In contrast, Br values rise rapidly to a sustained peak  
240 between c. 380 and 200 cal a BP.

241

## 242 **Discussion**

243 The down-core variations in Br and MSW indicate that changes in Br concentrations likely  
244 reflect longer-term changes in storminess in the NE Atlantic rather than biogenic processes  
245 within the peat bog. Therefore, our ~8000 year palaeo-wetness and storminess record from  
246 Shebster, Northern Scotland, can be interpreted alongside other key proxy records from  
247 around the North Atlantic to place the inferred palaeoenvironmental trends in a wider  
248 context of Holocene atmospheric circulation changes. These proxy records include: a 5000  
249 year glacier record from Folgefanna in Southern Norway (Bakke *et al.*, 2008); a  
250 reconstructed 5000 year NAO index based on a lake-sediment core in SW Greenland (Olsen  
251 *et al.*, 2012); a Scottish speleothem record (Baker *et al.*, 2015); and an Iberian speleothem  
252 record (Walkzak *et al.*, 2015) (Fig. 4). Variations in speleothem laminae thickness provide an  
253 annual growth-rate record that can be used as a proxy for past climate and environmental  
254 change. Growth rates are determined by changes in precipitation and higher growth rates  
255 suggest warmer and wetter conditions (positive NAO state) whereas low growth rates are

256 associated with colder and drier conditions (negative NAO state) (Baker *et al.*, 2015). The  
257 NAO index based on a south-west Greenland lake-sediment core is reconstructed from  
258 deep-water anoxia data (Olsen *et al.*, 2012). A negative NAO is associated with above  
259 average temperatures and below average winter precipitation, leading to earlier ice melt  
260 and allows stronger vertical mixing of the water column. This weakens thermal stratification  
261 and hence increases oxygen transfer into the deep-water zone, with associated implications  
262 for redox processes. A positive NAO, associated with colder conditions, leads to later ice  
263 melt, which coincides with maximum solar radiation and results in limited water column  
264 mixing. This leads to the rapid onset of thermal stratification, and hence maintenance of  
265 hypoxic conditions. Deep-water anoxia can alter cycling of redox-sensitive elements. The  
266 Mn/Fe ratio reflects the strength of seasonal thermal stratification and is therefore a proxy  
267 for dominant NAO circulation patterns. A higher Mn/Fe ratio and carbonate concentration  
268 reflects predominantly weaker stratification and is associated with negative NAO conditions,  
269 whereas a lower Mn/Fe ratio and carbonate concentration reflects stronger stratification  
270 and is associated with positive NAO conditions.

271

272 SH-1 8210 – 7400 cal a BP: To avoid the influence of any mineral material from the underlying  
273 lacustrine sediments the degree of peat humification was not analysed at the base of the peat  
274 (608 cm). The lowest part of the available record is characterised by several high magnitude  
275 fluctuations in wetness and storminess. Although the base of the analysed peat record starts  
276 at c. 8200 cal a BP, neither the Br record nor the MSW data completely capture the 8.2ka  
277 event, expressed as a marked rapid negative temperature anomaly across much of the  
278 Northern Hemisphere (Larsen *et al.*, 2012; Tipping *et al.*, 2012). However, SH-1 is dominated  
279 by a large Br positive anomaly centred at c. 7800 cal a BP, suggesting a period of enhanced

280 storminess lasting c. 300-400 years. By contrast, the humification record at this time suggests  
281 conditions of below-average wetness. This anti-phase relationship between MSW and Br  
282 appears paradoxical, but may suggest that these storms were cold, moisture-starved Polar  
283 vortex systems rather than moisture-bearing westerly winds. This is supported by the Iberian  
284 speleothem record, which shows a stable, positive record indicating warmer and wetter  
285 conditions. Rainfall in southern Iberia was more evenly distributed throughout the year,  
286 typical of a more temperate climate lacking a clear dry season (Walczak *et al.*, 2015) and may  
287 indicate a more southerly position of the jet stream and, therefore, a persistent negative NAO  
288 phase (phase B1, Fig. 1).

289

290 SH-2 7400-5270 cal a BP: After c. 7400 cal a BP there was a marked increase in MSW at  
291 Shebster and although the values fluctuate during the period between c. 7400 and 6200 cal a  
292 BP, they remain high suggesting the persistence of wetter conditions. However, Br values  
293 decrease from the initial peak in zone SH-1 which may suggest that although this zone reflects  
294 wetter conditions storminess was less intense than in SH-1. This period probably indicates a  
295 northerly migration of the jet-stream-driven westerly winds accompanied by a movement of  
296 the North Atlantic storm tracks to a position located over Northern Scotland. This atmospheric  
297 circulation pattern is best described by the positive mode of the NAO (phase A, Fig. 1).

298

299 In the second half of SH-2, from c. 6200 to 5270 cal a BP, MSW continues to reflect increased  
300 and more sustained wetter conditions. At the same time, Br values remain high indicating  
301 higher levels of storminess throughout this period. A pronounced peak in storminess occurs  
302 in zone SH-2 between c. 6145 and 5700 cal a BP. It is not certain what might have caused this  
303 ~400-year window of increased storminess, during a period of relatively wetter but more

304 stable climatic conditions. The Iberian speleothem record is characterised by a decline in  
305 growth rates between 6100 and 5300 cal a BP suggesting decreased moisture availability  
306 (Walczak *et al.*, 2015) and this is consistent with a stronger polar-front jet stream bringing an  
307 increase in the number and intensity of storms tracking over Northern Scotland (i.e. a strongly  
308 positive NAO mode).

309

310 SH-3 5270-4000 cal a BP: Between c. 5300 and 4000 cal a BP, MSW and Br values reflect a  
311 synchronised period of gradual and near-continuous decline in both precipitation and  
312 storminess over Northern Scotland. Several proxy records reflect a mixed climate signal at  
313 this time. The glacier-ELA-reconstructed winter precipitation record from Bakke *et al.* (2005)  
314 indicates a comparable near-continuous decrease in wetness over most of this period (c.  
315 5000-4000 cal a BP) and is consistent with the Iberian speleothem record which also shows a  
316 shift to drier conditions with the exception of an increase in wetness at c. 4200 cal a BP. This  
317 climate period is also captured by the earliest part of the SW Greenland lake-sediment-  
318 reconstructed NAO index, which shows a sustained positive NAO phase between c. 5200 and  
319 4400 cal a BP (Olsen *et al.*, 2012). These climatic conditions are all compatible with a period  
320 of geographically unstable jet stream position and/or declining jet stream strength bringing  
321 generally warmer, drier summer conditions to NW Europe accompanied by a decline in  
322 cyclogenesis with fewer storms tracking across northern Scotland. After c. 4400 cal a BP, the  
323 reconstructed NAO index (Olsen *et al.*, 2012) enters a relatively neutral phase consistent with  
324 a decrease in jet stream vigour, at a time when the Shebster peat record indicates steadily  
325 decreasing North Atlantic storm activity.

326

327 SH-4 4000-3300 cal a BP: This period marks the most striking departure in the Shebster peat  
328 record when MSW and Br values are at their lowest for the entire ~ 8000-year record. We  
329 relate these values to a sustained period of relatively drier climate and greatly reduced  
330 storminess following on from the decline in storminess seen in the preceding millennium (c.  
331 5300-4000 cal a BP; SH-3). A marked decrease in North Atlantic storminess in Northern  
332 Scotland could be associated with two different atmospheric circulation scenarios: (1)  
333 westerly wind and storm-track migration to a more southerly latitude (ca. 40°N) equating to  
334 a strongly negative winter NAO phase; (2) reduced jet stream strength and a low-value or  
335 neutral NAO phase. This period of unusual drier and calmer climate identified in the Shebster  
336 peat record is not restricted to Caithness, but is probably the expression of a pan-  
337 European/North Atlantic event seen widely in other Holocene palaeo-climate proxies. Peat  
338 surface-wetness records from a composite of 12 sites in Northern Britain (Charman *et al.*,  
339 2012) show a period of considerably decreased wetness from c. 3900 to 3400 cal a BP, the  
340 most pronounced in the mid to Late Holocene (interrupted by a brief increase in wetness at  
341 c. 3750 cal a BP). In southern Europe, often in antiphase with the climate of northern Britain,  
342 Mediterranean records from south-eastern Italy to south-western France record a period of  
343 relatively drier conditions between c. 4000 and 3400 cal a BP (e.g. Di Rita and Magri, 2009;  
344 Genty *et al.*, 2006; Walczak *et al.*, 2015), and this can also be seen in the Iberian speleothem  
345 record. Further afield, in continental North America and Mexico declining monsoon strength  
346 are recorded in a number of geographically diverse proxies from c. 4200 to 3500 cal a BP  
347 (Booth *et al.*, 2005; Metcalfe *et al.*, 2015). This is also coincident with the marked southerly  
348 migration of the ITCZ (c. 4000 cal a BP) seen in a number of low-latitude records, including  
349 the high-resolution Cariaco Basin (Haug *et al.*, 2001; Metcalfe *et al.*, 2015). Closer to Scotland,  
350 the same SH-3 time interval (c. 4000-3300 cal a BP) sees lower than present precipitation in



351 the Norwegian glacier record (Bakke *et al.*, 2005); whilst temperatures in south-west Ireland  
352 inferred from speleothems show a broad thermal minimum c. 3800 to 3400 cal a BP  
353 (McDermott *et al.*, 2001). It is notable that this period is also characterised by a marked  
354 negative departure in chlorine in the GISP2 record, inferred as a weakening of the Icelandic  
355 Low pressure system between c. 4500 and 3600 cal a BP (O'Brien *et al.*, 1995; Mayewski *et*  
356 *al.*, 2004).

357

358 The collected multi-proxy evidence from both sides of the North Atlantic points towards jet  
359 stream weakening during SH-4, leading to a decrease in cyclonic activity which reaches a  
360 minimum at c. 3800 cal a BP. Negative NAO conditions normally result in increased rainfall  
361 and storminess over southern Europe (e.g. Hurrell *et al.*, 2003; Pinto *et al.*, 2009), something  
362 that is not seen in most of the proxy records between c. 4000 and 3300 cal a BP (see above).  
363 Secondly, negative NAO phases have been strongly linked with meridional airflow and strong  
364 temperature contrasts causing enhanced but intermittent cyclogenesis in north-west Europe  
365 (Trouet *et al.*, 2012; Vliet-Lanoë *et al.*, 2014). Again, this is not evident in the Shebster record  
366 during SH-4, with storm-driven Br values reaching their 8000-year minimum within this time  
367 window. However, these observations, in combination with a prolonged neutral phase of the  
368 reconstructed NAO index (Olsen *et al.*, 2012), are entirely consistent with a decrease in jet  
369 stream vigour during SH-4. We would expect that this period experienced considerably  
370 reduced westerly (zonal) airflow at 50-60°N, accompanied by a higher incidence of quasi-  
371 stationary high-pressure systems over Northern Europe. There is evidence from the Shebster  
372 Br and MSW data that this c. 700-year period of subdued westerly winds (reduced jet stream  
373 vigour) and cyclogenesis over northern Scotland is the ultimate expression of a declining trend  
374 in storminess and wetness that started at c. 4500 cal a BP (in SH-3), coincident with the switch

375 from positive to low-value or neutral NAO values (<1.0) in the Greenland sediment record  
376 (Olsen *et al.*, 2012).

377

378 SH-5 3300 – 2400 cal a BP: A marked broadly synchronous increase in MSW and Br values at  
379 c. 3200-3300 cal a BP indicates the return to wet and stormy conditions in northern Scotland.  
380 This period (SH-5) is characterised by generally increasing MSW levels throughout (c. 3300-  
381 2400 cal a BP) and a relatively high but fluctuating storminess index. Supporting proxy data  
382 suggest more vigorous cyclogenesis, increased precipitation and raised water tables in north-  
383 west Europe at this time (Hughes *et al.*, 2000; Charman, 2010; Swindles *et al.*, 2007; Oldfield  
384 *et al.*, 2010), although the reconstructed NAO index displays a strong fluctuation from initially  
385 positive (c. 3300-3000 cal BP) to strongly negative values (c. 3000-2400 cal a BP) (Olsen *et al.*,  
386 2010). A marked concomitant rise in air temperatures and winter precipitation, seen in the  
387 Irish speleothem, Norwegian glacier and Iberian speleothem proxy-records (Fig 4) between c.  
388 3300 and 2700 cal a BP would also suggest a return to more dynamic atmospheric circulation  
389 patterns over north-west Europe with strongly zonal moisture-bearing winds and more  
390 moderate levels of cyclogenesis.

391

392 The most sustained period of negative NAO in the Greenland lake-sediment record is  
393 synchronous with an increase in MSW at Shebster (c. 2800-2400 cal a BP). This probably  
394 relates to a strengthening of the westerly winds (after the quiescent SH-4 phase) and a mean  
395 storm track positioned to the south of Scotland, consistent with the relative decrease in  
396 storminess at this time. The annually resolved north-west Scotland speleothem record also  
397 starts during this time (Baker *et al.*, 2015). Although no overall trend in the composite  
398 speleothem climate-index is apparent during the first ~500 years, relatively high-magnitude

399 peaks in speleothem growth rates at c. 2900 and 2600 cal a BP probably reflect decadal to  
400 centennial periods of higher precipitation in northern Scotland (Baker *et al.*, 2015).

401

402 At c. 3000 cal a BP glaciers become permanently established at some marginal sites in Iceland,  
403 Norway and southern Greenland for the first time since their complete disappearance in the  
404 early Holocene (c. 8000-7000 cal a BP) (Andresen & Bjork, 2005; Balascio *et al.*, 2015; Larsen  
405 *et al.*, 2012). Numerous other studies have linked this renewed ice growth, or Neoglaciation,  
406 with a shift towards wetter and/or cooler climate in Northern Hemisphere higher latitudes  
407 after c. 4200 cal a BP (Blaauw *et al.*, 2004; Swindles *et al.*, 2007; Wang *et al.*, 2012).

408

409 SH-6 2400-1400 cal a BP: During this period MSW at Shebster remains relatively high whilst  
410 Br levels are somewhat subdued (close to, but slightly below the 8000-year mean),  
411 continuing the long-term trend established in SH-5. The north-west Scotland speleothem  
412 record exhibits high growth rates suggesting moist but more stable climatic conditions.  
413 Elsewhere around Europe this millennium is synonymous with the 'Roman Warm Period'  
414 (2500-1600 cal a BP) (Wang *et al.*, 2012) and is characterised by a predominantly positive  
415 (>1.0) NAO index in Greenland (Olsen *et al.*, 2012). This strong pressure dipole, but relatively  
416 stable low-storm index state, suggests a poleward shift of the westerly storm tracks to a  
417 position between Iceland and Scotland, as seen during positive NAO summers. However, the  
418 low storm index suggests a more complex relationship, possibly with an increased polar  
419 front latitudinal range in winter with storms tracking to the south of northern Scotland.  
420 Support for this hypothesis comes from a peat record from Cors Fochno, mid Wales where  
421 sustained higher Br values between c. 2200 and 1600 cal a BP suggest that although the

422 Roman Warm period was comparatively dry at Shebster in Northern Scotland, North  
423 Atlantic storms still tracked across central and southern Britain with relatively high  
424 frequency (Orme *et al.*, 2015).

425

426 SH-7 1400 – 600 cal a BP: This period includes the Medieval Climate Anomaly (MCA: 700-1100  
427 cal a BP; Mann and Jones, 2003) and is characterised at Shebster by higher but variable MSW  
428 alongside relatively higher and variable Br levels in the peat record. Together they suggest a  
429 wetter and stormier period in Northern Scotland than the previous millennium (SH-6) which  
430 is consistent with the unusually long and unbroken, strongly positive, NAO phase (Trouet *et*  
431 *al.*, 2009). This is seen in the Greenland lake-sediment record from c. 1400 to 600 cal a BP  
432 (Olsen *et al.*, 2012). A positive NAO mode is normally associated with a vigorous jet stream  
433 and a North Atlantic winter storm track focused between 55-60°N (at the latitude of northern  
434 mainland Scotland) (Hurrell *et al.*, 2003; Woollings *et al.*, 2008, 2010). This circulation pattern  
435 is supported by several other palaeoenvironmental proxies from the British Isles and adjacent  
436 areas. Firstly, the composite British peat-surface wetness record compiled by Charman (2010)  
437 shows a continuous phase of elevated water tables spanning the entire 800-year period with  
438 a peak c. 1100-1200 cal a BP. Secondly, the Irish speleothem record shows several centuries  
439 of increasing above-average (inferred) temperatures, with a peak c. 700-900 cal a BP  
440 (McDermott *et al.*, 2001). Thirdly, the winter moisture index from Norwegian glaciers shows  
441 well above-average precipitation (120-140% present day) in this time interval (Bakke *et al.*,  
442 2008). Fourthly, the occurrence of outsized wave-transported boulders (cliff-top storm  
443 deposits) 15-60 m above sea level in Shetland, northern Scotland, dated to between c. 1300  
444 and 800 cal a BP (Hansom and Hall, 2009), indicate enhanced storminess at ~60°N. Finally,  
445 lower values of Br at Cors Fochno peat bog, relative to the preceding period (Orme *et al.*,

446 2015), suggest that the main westerly storm tracks were not focused at the latitude of mid  
447 Wales (52°N) but further north over Scotland. However, more complexity is introduced when  
448 comparing these proxy records with growth rates from the north-west Scotland speleothem  
449 record. Baker *et al.* (2015) reconstruct strongly negative NAO-like conditions from c. 1400 to  
450 1100 cal a BP, at which point the trend is reversed and their reconstruction shows a strongly  
451 positive phase throughout the MCA, similar to the Olsen *et al.* (2012) NAO record. Therefore,  
452 we interpret the MCA period to be one of a strong polar-front jet stream and enhanced  
453 cyclogenesis, bringing westerly storms tracking across northern Scotland (57-60°N). Although  
454 the variable antiphase relationship between MSW and Br records at Shebster perhaps  
455 suggest, at times, decreased storm frequency but higher storm intensity across the northern  
456 British Isles, consistent with the generation of high-energy storm deposits around northern  
457 Scotland's coasts (Hansom and Hall, 2009).

458

459 SH-8 600-0 cal a BP: The most recent period captured in the Shebster peat record spans from  
460 c. 600 to 100 cal a BP and almost exactly corresponds to the Little Ice Age (LIA: c. 150-700 cal  
461 a BP; Mann and Jones, 2003). This period is characterised at Shebster by high but variable  
462 MSW and generally high Br values, indicating increased wetness and storminess for much of  
463 this 500-year window. A notable exception is the period between c. 100 and 200 cal a BP  
464 when Br (i.e. storminess) is subdued with levels equivalent to SH-6. However, the cause of  
465 the LIA cooling (and/or any associated storminess) has been the source of considerable  
466 research and debate (Lamb, 1995; Orme *et al.*, 2016; Trouet *et al.*, 2012). A clear LIA signal is  
467 seen in the proxy-reconstructed NAO indices of Olsen *et al.* (2012) and Baker *et al.* (2015),  
468 where an abrupt shift from strongly positive to negative NAO occurs at c. 600 cal a BP in both  
469 records. The shift is larger and more sustained in the reconstruction provided by Baker *et al.*

470 (2015). The record suggests that this dominantly negative NAO phase was associated with a  
471 vigorous jet stream, a higher incidence of moisture-bearing winds and a higher frequency of  
472 storms generally tracking across the latitude of Northern Britain (55-60°N) for much of the LIA  
473 (c.100-600 cal a BP). The normal negative NAO configuration involves a significant southward  
474 shift in dominant westerly winds and storm tracks, to the latitude of southern France,  
475 northern Iberia and the western Alps (40-45°N) (Woollings *et al.*, 2008, 2010). However, other  
476 records from around Scotland show with a high level of certainty that the LIA period (esp.  
477 from 400-100 BP) was one of periodically enhanced storminess, increased sea state and wave  
478 activity, and generally disrupted weather patterns (Sommerville *et al.*, 2003; McIlvenny *et al.*,  
479 2013; Orme *et al.*, 2016). These features are the hallmarks of an unusually turbulent period  
480 of atmospheric circulation, typically associated with disturbed jet stream strength and an  
481 unstable location (switching from zonal to meridional flow pattern), consistent with variable  
482 but high levels of Br-inferred storminess at Shebster (this study) and to a lesser degree at Cors  
483 Fochno (Orme *et al.*, 2015) during the second half of the LIA. However, the speleothem and  
484 MSW records reflect a shift to relatively drier although perhaps less stable conditions. Again  
485 the contrast between the records of storminess and local wetness is probably due to the LIA  
486 being dominated by overall colder and drier conditions but affected by lower-frequency  
487 higher-intensity storm events (supporting the findings of Trouet *et al.*, 2012).

488

## 489 **Conclusions**

490 The Shebster climate record provides insights into the timing and nature of North Atlantic  
491 climate changes and is a significant advance to the existing records in that it spans much of  
492 the Holocene. The combined Br and MSW records highlight the millennial to centennial  
493 scale changes in the position of the polar jet stream – a significant driver of environmental

494 change in northern Scotland and the wider North Atlantic region. The Shebster climate  
495 record is consistent with the Norwegian glacier record, Greenland sediment-inferred NAO  
496 index, Scottish speleothem record and Iberian speleothem record but most importantly  
497 advances our understanding of the development and fluctuations of the NAO from the early  
498 Holocene. We infer from the data that periods of high Br and MSW levels probably relate to  
499 a jet stream position over Northern Scotland and, therefore, increased storminess and a  
500 positive NAO mode. Periods of reduced Br and mire wetness levels probably relate to a  
501 more southerly position of the jet stream and, therefore, a decline in storminess and a  
502 negative NAO. Between c. 4000 and 3300 cal a BP there are very low levels of Br and mire  
503 wetness consistent with a drier period across much of the northern hemisphere which may  
504 relate to a neutral NAO state and a weaker jet stream. However, subtle differences between  
505 these two proxies suggest that single indicators of storminess may not be sufficient to  
506 reconstruct changes in jet stream movement and NAO index. These differences also suggest  
507 that higher intensity but perhaps less frequent periods of storminess are not necessarily  
508 associated with a wetter climate, which may be exemplified during the Little Ice Age. This  
509 work shows that important high-resolution palaeoenvironmental information can be  
510 gleaned by XRF-analysis of peat accumulations in cold-temperate climates. Furthermore,  
511 these analyses in combination with other established techniques offer a novel and under-  
512 used way to examine the climate record of the recent past on a decadal to millennial scale.

513

514 *Acknowledgements* The authors wish to thank the NERC-BGS opportunities fund and  
515 support from Dounreay Site Restoration Ltd, which led to the development of this project.  
516 HS was supported by a NERC-BUFI – University of Stirling joint studentship (NE/K501156/1).  
517 We would like to thank Dr Andrew Finlayson, Dr Mary McCulloch, Natasha Rolph and James

518 Blaikie for invaluable assistance in the field. We are also grateful to Dr Chris Hayward for his  
519 guidance and support for our use of the electron microprobe at the School of GeoSciences,  
520 The University of Edinburgh. Two anonymous reviewers are thanked for their comments.

521

## 522 **References**

523 Alexander LV, Tett SFB. 2005. Recent observed changes in severe storms over the United  
524 Kingdom and Iceland. *Geophysical Research Letters* **32** : 1-4.

525

526 Allan R, Tett S, Alexander L. 2009. Fluctuations in autumn-winter severe storms over the  
527 British Isles: 1920 to present. *International Journal of Climatology* **29** : 357-371.

528

529 Andresen CS, Björck S. 2005. Holocene climate variability in the Denmark Strait region.  
530 *Geografiska Annalar* **1**: 159-174.

531

532 Andresen CS, Bond G, Kuijpers A, Knutz PC, Björck S. 2005. Holocene climate variability at  
533 multidecadal time scales detected by sedimentological indicators in a shelf core NW off  
534 Iceland. *Marine Geology* **214**: 323-338.

535

536 Athanasiadis PJ, Wallace JM, Wettstein JJ. 2010. Patterns of jet stream wintertime variability  
537 and their relationship to the storm tracks. *Journal of Atmospheric Sciences* **67**: 1361-1381.

538

539 Auton CA, Gillespie MR, Lott G.K, McKervey JA, Milodowski AE, Stephenson MH. 2005.

540 Palynological and petrological constraints on correlation of Devonian strata across the



541 Dounreay district, BGS Commissioned Report CR/05/009. British Geological Survey,  
542 Edinburgh.

543

544 Bakke J, Lie Ø, Nesje A, Dahl SO, Paasche Ø. 2005. Utilizing physical sediment variability in  
545 glacier-fed lakes for continuous glacier reconstructions during the Holocene, northern  
546 Folgefonna, western Norway. *Journal of Quaternary Science* **15**: 161-176.

547

548 Bakke J, Lie Ø, Dahl SO, Nesje A, Bjune AE. 2008. Strength and spatial patterns of the  
549 Holocene wintertime westerlies in the NE Atlantic region. *Global and Planetary Change* **60**:  
550 28-41.

551

552 Baker A, Hellstrom J, Kelly B, Mariethoz G, Trouet V. 2015. A composite annual-resolution  
553 stalagmite record of North Atlantic climate over the last three millennia. *Scientific Reports* **5**:  
554 doi:10.1038/srep10307.

555

556 Balascio NL, D'Andrea WJ, Bradley RS. 2015. Glacier response to North Atlantic climate  
557 variability during the Holocene. *Climate of the Past* **11**: 1587-1598.

558

559 Biester H, Keppler F, Putschew A, Martinez-Cortizas A, Petri M. 2004. Halogen retention,  
560 organohalogens, and the role of organic matter decomposition on halogen enrichment in  
561 two Chilean peat bogs. *Environmental Science and Technology* **38**: 1984– 1991.

562

563 Blaauw M, Van Geel B, Van der Plicht J. 2004. Solar forcing of climatic changes during the  
564 mid-Holocene: indications from raised bogs in the Netherlands. *The Holocene* **14**: 1-35.

565

566 Blaauw M, Christen JA. 2011. Flexible paleoclimate age-depth models using an  
567 autoregressive gamma process. *Bayesian Analysis* **6**: 457-474.

568

569 Blackford JJ, 1993. Peat bogs as sources of proxy climatic data: past approaches and future  
570 research. In *Climatic change and human impact on the landscape. Studies in palaeoecology  
571 and environmental archaeology*, Chambers FM (ed.). Chapman & Hall: London; 47-56.

572

573 Booth RK, Jackson SL, Forman JE, Kutzbach EA, Bettis III, Kreig J, Wright DK. 2005. A severe  
574 centennial-scale drought in continental North America 4200 years ago and apparent global  
575 linkages. *The Holocene* **15**: 321-328.

576

577 Charman DJ, Blundell A, Chiverrell RC, Hendon D, Langdon PG. 2006. Compilation of non-  
578 annually resolved Holocene proxy climate records: stacked Holocene peatland palaeo-water  
579 table reconstructions from northern Britain. *Quaternary Science Reviews* **25**: 336–350.

580

581 Charman DJ, Barber KE, Blaauw M, Langdon PG, Mauquoy D, Daley TJ, Hughes PDM,  
582 Karofeld E. 2009. Climate drivers for peatland paleoclimate reconstructions. *The Holocene*  
583 **17**: 217-227.

584

585 Charman DJ. 2010. Centennial climate variability in the British Isles during the mid-late  
586 Holocene. *Quaternary Science Reviews* **29**: 1539-1554.

587

588 Cheng X, Xie S-P, Tokinaga H, Du Y. 2011. Interannual Variability of High-Wind Occurrence  
589 over the North Atlantic. *Journal of Climate* **24**: 6515-6527.

590

591 Clarke M, Rendell H, Tastet J-P. 2002. Late-Holocene sand invasion and North Atlantic  
592 storminess along the Aquitaine coast, southwest France. *The Holocene* **12**: 231–238.

593

594 Clarke ML, Rendell HM. 2009. The impact of North Atlantic storminess on western European  
595 coasts: A review. *Quaternary International* **195**: 31-41.

596

597 Dawson AG, Elliot L, Mayewski P, Lockett P, Noone S, Hickey K, Holt T, Wadhams P, Foster I.  
598 2003. Late Holocene North Atlantic climate ‘seesaws’, storminess changes and Greenland  
599 ice sheet (GISP2) paleoclimates. *The Holocene* **13**: 381-392.

600

601 Dawson AG, McIlveny J, Warren J. 2010. Winter Gale Day Frequency in Shetland and  
602 Faeroes, AD 1866–1905: Links to Sea Ice History and the North Atlantic Oscillation. *Scottish*  
603 *Geographical Journal*, **126**: 141 - 152.

604

605 De Jong R, Björck S, Björckman L, Clemmensen LB. 2006. Storminess variation during the last  
606 6500 years as reconstructed from an ombotrophic peat bog in Halland, Southwest Sweden.  
607 *Journal of Quaternary Science* **21**: 905-919.

608

609 De la Vega-Leinert AC, Keen DH, Jones R L, Wells JM, Smith DE. 2000, Mid-Holocene  
610 environmental changes in the Bay of Skail, Mainland Orkney, Scotland: an integrated

611 geomorphological, sedimentological and stratigraphical study. *Journal of Quaternary*  
612 *Science*, 15: 509–528.

613

614 Di Rita F, Magri D. 2009. Holocene drought, deforestation and evergreen vegetation  
615 development in the central Mediterranean: A 5500 year record from Lago Alimini, Piccolo,  
616 Apulia, southeast Italy. *The Holocene* **19**: 295-306.

617

618 Dugmore AJ, Larsen G, Newton, AJ. 1995a. Seven tephra isochrones in Scotland. *The*  
619 *Holocene* **5**: 257-266.

620

621 Dugmore AJ, Cook GT, Shore JS, Newton AJ, Edwards KJ, Larsen G. 1995b. Radiocarbon  
622 Dating Tephra Layers in Britain and Iceland. *Radiocarbon* **37**: 379-388.

623

624 Genty D, Blamart D, Ghaleb B, Plagnes V, Causse C, Bakalowicz M, Melières MA, Zouari K,  
625 Chkir N. 2006. Timing and Dynamics of the Last Deglaciation from European and North  
626 African  $\delta^{13}\text{C}$  stalagmite profiles – Comparison with South-Hemisphere stalagmite records.  
627 *Quaternary Science Review* **25**: 2118-2142.

628

629 Hanna E, Cappelen J, Allan R, Jónsson T, Le Blaq F, Lillington T, Hickey K. 2008. New insights  
630 into North European and North Atlantic surface pressure variability, storminess, and related  
631 climate change since 1830. *Journal of Climate* **21**: 6739-6766.

632

633 Hansom JD, Hall AM. 2009. Magnitude and frequency of extra-tropical North Atlantic  
634 cyclones: A chronology from cliff-top storm deposits. *Quaternary International* **195**: 42-52.

635

636 Haug GH, Hughen KA, Sigman DM, Petersen LC, Röhl U. 2001. Southward migration of the  
637 Intertropical Convergence Zone through the Holocene. *Science* **293**: 1304-1308.

638

639 Hayward C. 2013. High spatial resolution electron probe microanalysis of tephras and melt  
640 inclusions without beam-induced chemical modification. *The Holocene* **22**: 119–125.

641

642 Hughes PDM, Mauquoy D, Barber KE, Langdon PG. 2000. Mire-development pathways and  
643 paleoclimatic records from a full Holocene peat archive at Walton Moss, Cumbria, England.  
644 *The Holocene* **10**: 465-479.

645

646 Hunt JB, Hill PG. 1993. Tephra geochemistry: a discussion of some persistent analytical  
647 problems. *The Holocene* **3**: 271-278.

648

649 Hurrell JW. 1995. Decadal Trends in the North Atlantic Oscillation: Regional Temperatures  
650 and Precipitation. *Science* **269** : 676-679.

651

652 Hurrell J W, Kushnir Y, Ottersen G, Visbeck M. 2003. An Overview of the North Atlantic  
653 Oscillation. In *The North Atlantic Oscillation: Climatic Significance and Environmental Impact*

654 Hurrell JW, Kushnir Y, Ottersen G, Visbeck M. (eds.). American Geophysical Union:  
655 Washington, D. C.; 1-35.

656

657 Larsen DJ, Miller GH, Geirsdóttir Á, Ólafsdóttir S. 2012. Non-linear Holocene climate  
658 evolution in the North Atlantic: a high-resolution, multi-proxy record of glacier activity and

659 environmental change from Hvítárvatn, central Iceland. *Quaternary Science Reviews* **39**: 14-  
660 25.

661

662 McDermott F, Matthey DP, Hawkesworth C. 2001. Centennial-scale Holocene climate  
663 variability revealed by a high-resolution speleothem delta O-18 record from SW Ireland.  
664 *Science* **294**: 1328–1331.

665

666 McIlvenny JD, Muller FLL, Dawson A. 2013. A 7600-year sedimentary record of climatic  
667 instability in Dunnet Bay, North Scotland. *Marine Geology* **335**: 100-113.

668

669 Mann ME, Jones PD. 2003. Global surface temperatures over the past two millennia.  
670 *Geophysical Research Letter*, **30**: 10.1029/2003GL017814.

671

672 Mauri A, Davis BAS, Collins PM, Kaplan JO. 2014. The influence of atmospheric circulation on  
673 the mid-Holocene climate of Europe: a data-model comparison. *Climates of the Past* **10**:  
674 1925–1938.

675

676 Mayewski PA, Rohling EE, Stager JC, Karlen W, Maasch KA, Meeker LD, Meyerson EA, Gasse  
677 F, Van Kreveld S, Holmgren K, Lee-Thorp J, Rosqvist G, Rack F, Staubwasser M, Schneider RR,  
678 Steig EJ. 2004. Holocene climate variability. *Quaternary Research* **62**: 243–255.

679

680 Metcalfe SE, Barron JA, Davies SJ. 2015. The Holocene history of the North American  
681 Monsoon: known knowns and known unknowns in understanding its spatial and temporal  
682 complexity. *Quaternary Science Reviews* **120**: 1-27.

683

684 Moreno j, Fatela F, Leorri E, Araújo MF, Moreno F, De la Rosa J, Freitas MC, Valente T,  
685 Corbett R. 2015. Bromine enrichment in marsh sediments as a marker of environmental  
686 changes driven by grand solar minima and anthropogenic activity (Caminha, NW of Portugal)  
687 *Science of the Total Environment* **506–507**: 554–566.

688

689 Newton AJ. 1996. Tephabase: A Tephrochronological Database. *Quaternary Newsletter* **78**:  
690 8-13.

691

692 O'Brien SR, Mayewski PA, Meeker LD, Meese DA, Twickler MS, Whitlow SI. 1995. Complexity  
693 of Holocene climate as reconstructed from a Greenland ice core. *Science* **270**: 1962–1964.

694

695 Oldfield F, Batterbee RW, Boyle JF, Cameron NG, Davis B, Evershed RP, McGovern AD, Jones  
696 V, Thompson R. 2010. Terrestrial and aquatic ecosystem responses to the late Holocene  
697 climate change recorded in the sediments of Lochan Uaine, Cairngorms, Scotland.  
698 *Quaternary Science Reviews* **29**: 1040-1054.

699

700 Olsen J, Anderson NJ, Knudsen MF. 2012. Variability of the North Atlantic Oscillation over  
701 the past 5200 years. *Nature Geoscience* **5**: 808–812.

702

703 Orme LC, Davies SJ, Duller GAT. 2015. Reconstructed centennial variability of Late Holocene  
704 storminess from Cors Fochno, Wales, UK. *Journal of Quaternary Science* **30**: 478-488.

705

706 Orme LC, Reinhardt L, Jones RT, Charman DJ, Barkwith A, Ellis MA. 2016. Aeolian sediment  
707 reconstructions from the Scottish Outer Hebrides: Late Holocene storminess and the role of  
708 the North Atlantic Oscillation. *Quaternary Science Reviews* **132**: 15-25.

709

710 Pinto JG, Zacharias S, Fink AH, Leckebusch GC, Ulbrich U. 2009. Factors contributing to the  
711 development of extreme North Atlantic cyclones and their relationship with the NAO.  
712 *Climate Dynamics* **32**: 711-737.

713

714 Reimer PJ, Bard E, Bayliss AJ, Beck W, Blackwell PG, Bronk Ramsey C, Buck CE, Cheng H,  
715 Edwards RL, Friedrich M, Grootes PM, Guilderson TP, Haflidason H, Hajdas I, Hatté C, Heaton  
716 TJ, Hoffmann DL, Hogg AG, Hughen KA, Kaiser KF, Kromer B, Manning SW, Niu M, Reimer  
717 RW, Richards DA, Marian Scott EM, Southon JR, Staff RA, Turney CSM, Van der Plicht J. 2013.  
718 INTCAL13 and MARINE13 Radiocarbon Age Calibration Curves 0–50,000 years cal. BP.  
719 *Radiocarbon* **55**: 1869–1887.

720

721 Sabatier P, Dezileau L, Colin C. 2012. 7000 years of paleostorm activity in the NW  
722 Mediterranean Sea in response to Holocene climate events. *Quaternary Research* **77**: 1–11.

723

724 Sander R, Keene WC, Pszenny AAP, Arimoto R, Ayers GP, Baboukas E, Cainey JM, Crutzen PJ,  
725 Duce RA, Hönninger G, Huebert BJ, Maenhaut W, Mihalopoulos N, Turekian VC, Van  
726 Dingenen R. 2003. Inorganic bromine in the marine boundary layer: a critical review.  
727 *Atmospheric Chemistry and Physics* **3**: 1301-1336

728



729 Stuiver M, Reimer PJ. 1993. Extended 14C database and revised CALIB radiocarbon  
730 calibration program. *Radiocarbon* **35**: 215-230.  
731

732 Swindles G, Plunkett G, Roe HM. 2007. A delayed response to solar forcing at 2800 cal. BP:  
733 multiproxy evidence from three Irish peatlands. *The Holocene* **17**: 177-182.  
734

735 Sommerville AA, Hansom JD, Sanderson DCW, Housley RA. 2003. Optically stimulated  
736 luminescence dating of large storm events in Northern Scotland. *Quaternary Science*  
737 *Reviews* **22**: 1085-1092.  
738

739 Strong C, Davis RE. 2008. Variability in the position and strength of winter jet stream cores  
740 related to Northern Hemisphere teleconnections. *Journal of Climatology* **21**: 584-592.  
741

742 Tipping R, Bradley R, Sanders J, McCulloch R, Wilson R. 2012. Moments of crisis: climate  
743 change in Scottish prehistory. *Society of Antiquaries of Scotland* **142**: 9-25.  
744

745 Tisdall E, McCulloch R, Sanderson D, Simpson I, Woodward N. 2013. Living with sand: A  
746 record of landscape change and storminess during the Bronze and Iron Ages Orkney,  
747 Scotland. *Quaternary International* **308-309**: 205-215.  
748

749 Trouet V, Esper J, Graham NE, Baker A, Scourse JD, Frank, DC. 2009. Persistent Positive  
750 North Atlantic Oscillation Mode Dominated the Medieval Climate Anomaly. *Science* **324**: 78-  
751 80  
752

753 Trouet V, Scourse JD, Raible CC. 2012. North Atlantic storminess and Atlantic Meridional  
754 Overturning Circulation during the last millennium: Reconciling contradictory proxy records  
755 of NAO variability. *Global and Planetary Change* **84-85**: 48-55.

756

757 Turner TE, Swindles GT, Roucoux KH. 2014. Late Holocene ecohydrological and carbon  
758 dynamics of a UK raised bog: impact of human activity and climate change. *Quaternary*  
759 *Science Reviews* **84**: 65-85.

760

761 Vliet-Lanoë B, Penaud AI, Hénaff A, Delacourt C, Fernane A, Goslin JRM, Hallégouët B, Le  
762 Cornec E. 2014. Middle-to-late Holocene storminess in Brittany (NW France): Part II – the  
763 chronology of events and climate forcing, *Holocene* **24**: 296-310.

764

765 Walczak IW, Baldini JUL, Baldini LM, McDermott F, Marsden S, Standish CD, Richards DA,  
766 Andreo B, Slater J. 2015. Reconstructing high-resolution climate using CT scanning of  
767 unsectioned stalagmites: A case study identifying the mid-Holocene onset of the  
768 Mediterranean climate in southern Iberia. *Quaternary Science Reviews* **127**: 117-128.

769

770 Wang XL, Zwiers FW, Swail VR, Feng Y. 2009. Trends and variability of storminess in the  
771 Northeast Atlantic region. 1874-2007. *Climate Dynamics* **33**: 1179-1195.

772

773 Wang T, Surge D, Mithen S. 2012. Seasonal temperature variability of the Neoglacial (3300–  
774 2500 BP) and Roman Warm Period (2500–1600 BP) reconstructed from oxygen isotope  
775 ratios of limpet shells (*Patella vulgata*), Northwest Scotland. *Palaeogeography,*  
776 *Palaeoclimatology, Palaeoecology* **317–318**: 104–113.

777

778 Woollings T, Hoskins B, Blackburn M, Berrisford P. 2008. A new Rossby wave-breaking  
779 interpretation of the North Atlantic Oscillation. *Journal of the Atmospheric Sciences* **65**: 609-  
780 626.

781

782 Woollings T, Hannachi A, Hoskins B. 2010. Variability of the North Atlantic eddy-driven jet  
783 stream. *Quarterly journal of the Royal Meteorological Society* **136**: 856-868.

784

785 Zaccone C, Cocozza C, Shotyk W, Miano TM. 2008. Humic acids role in Br accumulation along  
786 two ombrotrophic peat bog profiles. *Geoderma*, **146**: 26-31.

787

788

## 789 **List of Figures**

790 Figure 1: The preferred positions of the Polar Front Jet Stream and the corresponding  
791 phases of the NAO). White lines - Polar Front (i.e. average southern winter limit of Polar air  
792 masses). Grey long-dashed line - mean position of jet stream core between 1958 and 2006  
793 (from Strong & Davis, 2008). Coloured arrows -- approximate position of Polar vortex winds  
794 (colours match storms). Mode A dominates during strongly positive NAO phases; mode B<sub>1</sub> or  
795 B<sub>2</sub> dominates during strongly negative NAO. Neutral NAO phase (neither positive or  
796 negative) equates to a weak jet stream, with much-reduced storm frequency probably along  
797 negative NAO tracks (B<sub>1</sub>, B<sub>2</sub>).

798

799 Figure 2: A) Location map showing the study site in Northern Scotland. B) Detailed map of  
800 peat coring site near the Burn of Shebster. [Grid ticks are in British National Grid.] C)

801 Average climatological conditions (1981-2010) at the nearest long-running weather station  
802 (Wick Airport; 58.454 N, 3.089 W; 36 m asl). Mean monthly air temperature (maximum and  
803 minimum) and normal wind speed envelope (at 10 m) plotted on the same axis. Mean  
804 monthly precipitation shown as blue bars. [Data from metoffice.gov.uk]. Note the marked  
805 seasonality in average wind strength, peaking in winter (Dec-Mar).

806

807 Figure 3: Shebster stratigraphy, LOI<sub>550</sub>, Mire Surface Wetness, Bromine (ratio of Br /  
808 Inc+Coh) and BACON age/depth model.

809

810 Figure 4: Shebster Mire Surface Wetness, Bromine, 5000-yr glacier record from Folgefanna  
811 in Southern Norway (Bakke *et al.*, 2008), reconstructed 5000-yr NAO index based on a lake-  
812 sediment core in SW Greenland (Olsen *et al.*, 2012), Scottish speleothem record (Baker *et al.*,  
813 2015) and Iberian speleothem record (Walkzak *et al.*, 2015). The Hekla 4 tephra layer is  
814 indicated by a grey dotted line.

815

## 816 **List of Tables**

817

818 Table 1: Radiocarbon dates and ages for the H4 tephra layer correlated to the Shebster record.  
819 <sup>14</sup>C dates have been calibrated using CALIB Rev. 7.10 (Stuiver and Reimer, 1993) and IntCal  
820 13.14c. (Reimer *et al.*, 2013).

821

822

Figure 1

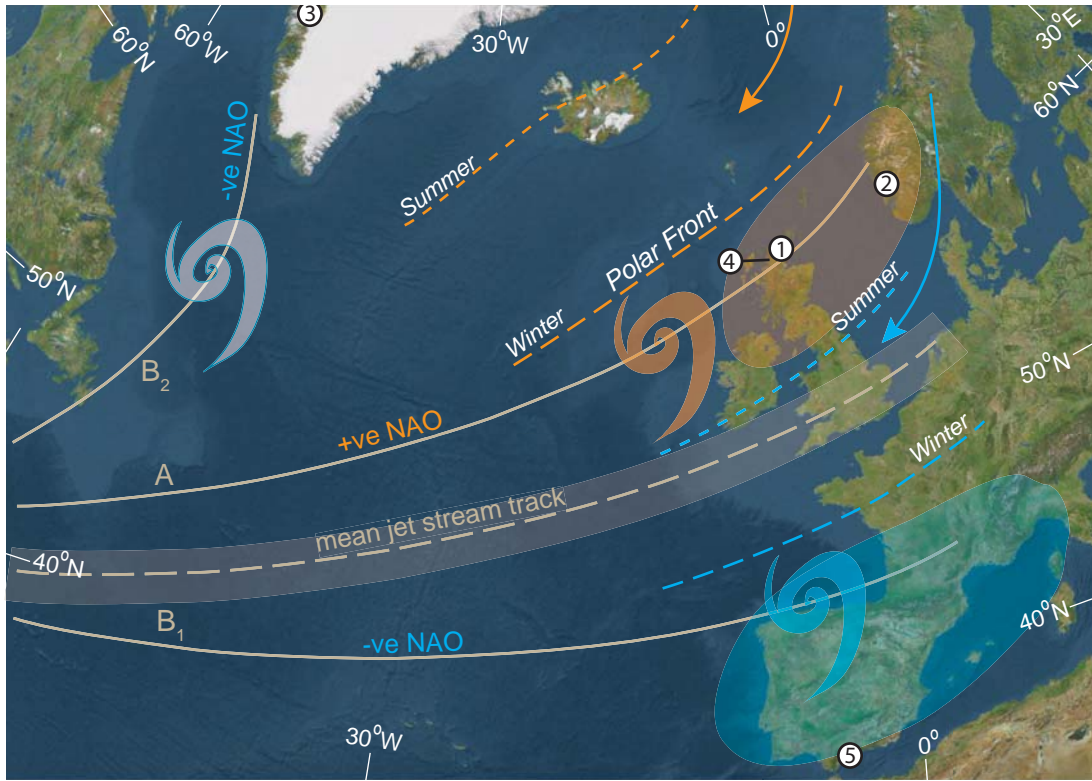


Figure 2

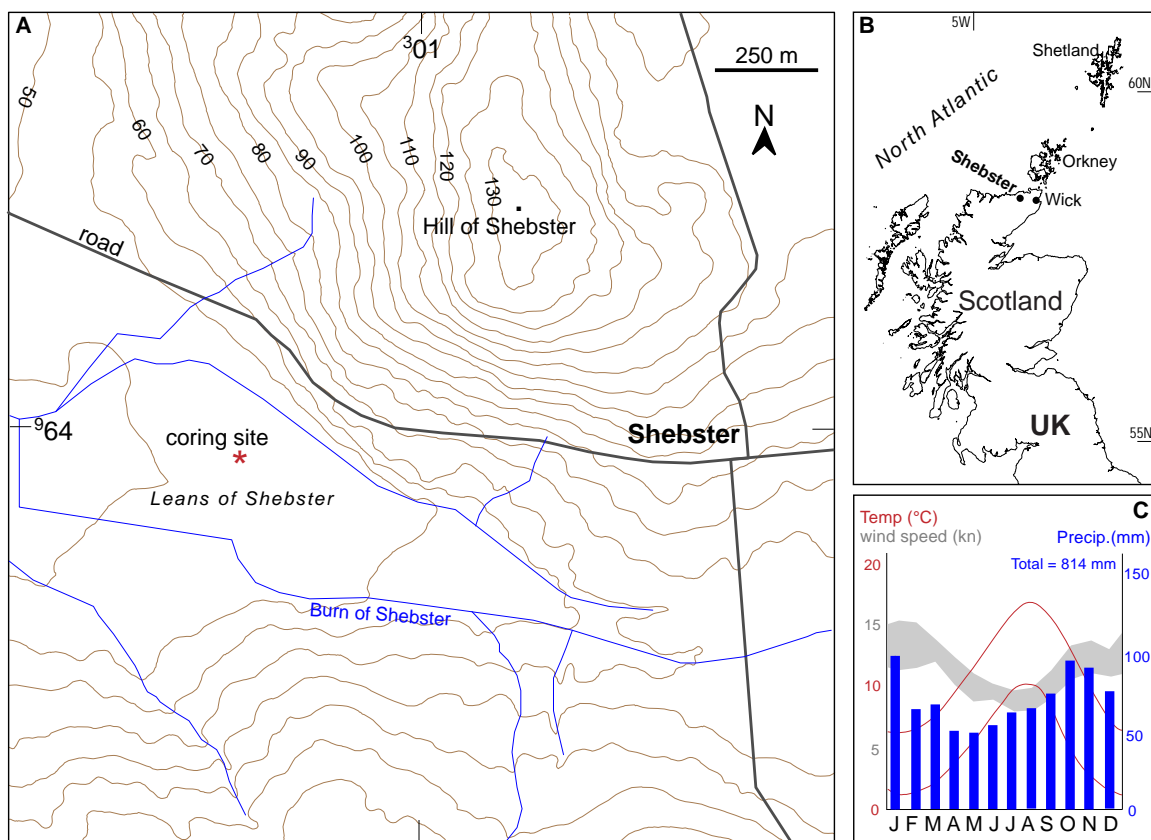


Figure 3

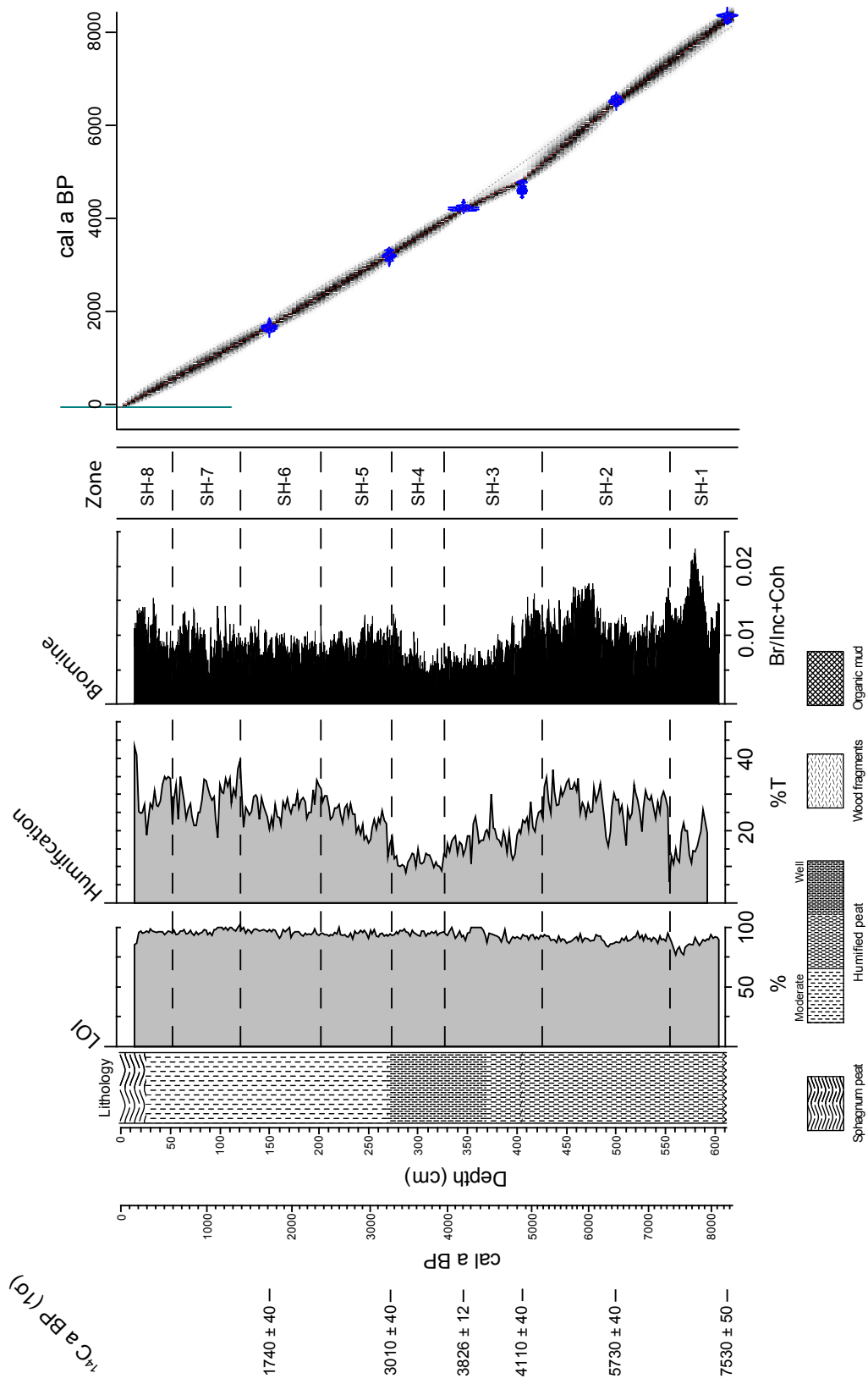


Figure 4

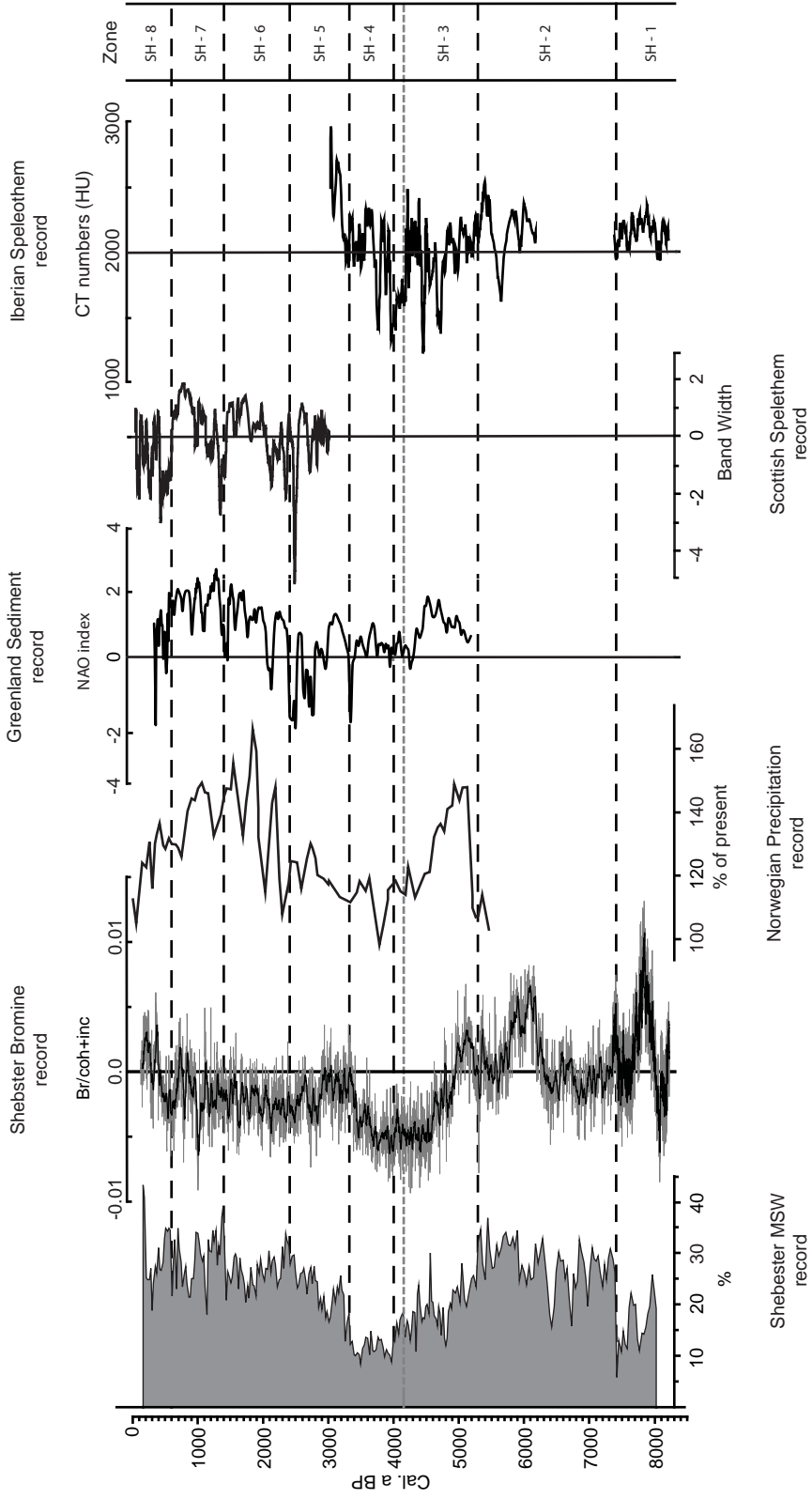




Table 1: Radiocarbon dates and ages for the H4 tephra layer correlated to the Shebster record. <sup>14</sup>C dates have been calibrated using CALIB Rev. 7.10 (Stuiver and Reimer, 1993) and IntCal 13.14c. (Reimer *et al.*, 2013).

Depth (cm)	<sup>14</sup> C a BP (1σ)	δ <sup>13</sup> C <sub>V-PDB</sub> ‰	cal a BP (1σ) <sup>2</sup>	Weighted Mean Age (cal a BP) <sup>3</sup>	Laboratory Code
150	1740 ± 40	-28.3	1606 – 1706	1679	Beta 251972
271	3010 ± 40	-28.0	3083 – 3322	3215	Beta 251973
346	3826 ± 12 <sup>1</sup>	n/a	4159 – 4241	4199	N/A
405	4110 ± 40	-29.4	4532 – 4802	4841	Beta 251974
500	5730 ± 40	-25.6	6454 – 6601	6507	Beta 251975
612	7530 ± 50	-24.7	8320 – 8403	8286	Beta 251976

<sup>1</sup> <sup>14</sup>C age for Hekla 4 cryptotephra layer (Dugmore *et al.*, 1995b)

<sup>2</sup> Calibrated ages produced using Calib Ver.7.1 (Stuiver and Reimer, 1993) and IntCal13 (Reimer *et al.*, 2013)

<sup>3</sup> Weighted mean ages produced using BACON Bayesian age-depth program (Blaauw and Christen, 2011)